Ferromagnetic Ordering in the Thallide $EuPdTl_2$

Rainer Kraft, Sudhindra Rayaprol, C. Peter Sebastian, and Rainer Pöttgen

Institut für Anorganische und Analytische Chemie and NRW Graduate School of Chemistry, Westfälische Wilhelms-Universität Münster, Corrensstraße 30, D-48149 Münster, Germany

Reprint requests to R. Pöttgen. E-mail: pottgen@uni-muenster.de

Z. Naturforsch. **61b,** 159 – 163 (2006); received January 5, 2006

The new thallide $EuPdTl_2$, synthesized from the elements in a sealed tantalum tube in a high-frequency furnace, was investigated by X-ray diffraction on powders and single crystals: $MgCuAl_2$ type, *Cmcm*, $Z = 4$, $a = 446.6(1)$, $b = 1076.7(2)$, $c = 812.0(2)$ pm, $wR2 = 0.0632$, 336 F^2 values, 16 variables. The structure can be considered as an orthorhombically distorted, palladium-filled variant of the binary Zintl phase $EuTl_2$. The palladium and thallium atoms build up a three-dimensional $[PdTl_2]$ polyanion with significant Pd–Tl (286 – 287 pm) and Tl–Tl (323 – 329 pm) interactions. The europium atoms fill distorted hexagonal channels of the $[PdTl_2]$ polyanion. Susceptibility measurements show a magnetic moment of 7.46(5) μ_B/Eu atom, indicative of divalent europium. $EuPdTl_2$ is a soft ferromagnet with a Curie temperature of $T_C = 12.5(5)$ K.

Key words: Thallide, Europium, Intermetallics, Crystal Chemistry, Magnetochemistry

Introduction

So far more than seventy aluminides, gallides, and indides with the orthorhombic $MgCuAl_2$ type structure [1, 2] have been reported. This structure type leaves great flexibility for bonding within the aluminium, gallium, and indium substructures. Depending on the size of the cation on the magnesium position, the $[TAl_2]$, $[TGa_2]$, and $[TIn_2]$ polyanionic networks (T = late transition metal) can be two- or three-dimensional. The crystal chemistry and physical properties of this family of compounds has been summarized in a recent review [3].

With the higher congener thallium, only the strontium based compounds $SrPdTl_2$ and $SrPtTl_2$ [4] have been reported. Property measurements on the palladium compound revealed fairly good metallic conductivity and simple Pauli paramagnetism. During our systematic investigations of structure-property relations of $MgCuAl_2$ type intermetallics [3] we succeeded in the preparation of $EuPdTl_2$ with the paramagnetic Eu^{2+} ions. The crystal chemistry and the magnetic properties of $EuPdTl_2$ are reported herein.

Experimental Section

Synthesis

Starting materials for the preparation of $EuPdTl_2$ were sublimed europium ingots (Johnson Matthey, $> 99.9\%$), palladium powder (Degussa-Hüls, *ca.* 200 mesh, $> 99.9\%$), and thallium granules (Johnson-Matthey, $\varnothing 1 - 5$ mm, kept under water). The elements were weighed in the ideal 1:1:2 atomic ratio and sealed in a tantalum tube [5] under an argon pressure of *ca.* 600 mbar. The argon was purified before over titanium sponge (900 K), silica gel, and molecular sieves. The tantalum tube was placed in a water-cooled sample chamber [6] of an induction furnace (Hüttinger Elektronik, Freiburg, Typ TIG 1.5/300) and first heated to *ca.* 1500 K for 5 min. The sample was then rapidly cooled to 900 K and kept at this temperature for another four hours. Finally the tube was quenched to room temperature by switching off the power of the generator. The temperature was controlled through a Sensor Therm Metis MS09 pyrometer with an accuracy of ± 30 K.

The sample could be separated quantitatively from the tantalum tube by mechanical fragmentation. No reaction of the sample with the crucible material was observed. Polycrystalline $EuPdTl_2$ was obtained as a silvery solid with metallic luster. $EuPdTl_2$ is sensitive to humidity and the sample was therefore kept in a Schlenk tube under argon prior to characterization.

The single crystal investigated on the diffractometer and the bulk sample were analyzed by EDX using a LEICA 420 I scanning electron microscope with EuF_3, Pd, and Tl as standards. The single crystal mounted on a quartz fibre was coated with a thin carbon film. EuF_3 and Pd were used as standards, but no standard was available for thallium. The EDX analyses (24 ± 2 at.-% Eu : 26 ± 2 at.-% Pd : 50 ± 2 at.-% Tl) revealed no impurity elements and was

Table 1. Crystal data and single crystal structure refinement of $EuPdTl_2$.

Empirical formula	$EuPdTl_2$
Formula weight [g/mol]	667.10
Unit cell dimensions [pm]	$a = 446.6(1)$
(Guinier data)	$b = 1076.7(2)$
	$c = 812.0(2)$
Cell volume / nm^3	$V = 0.3905$
Pearson symbol	oC16
Structure type	$MgCuAl_2$
Space group	*Cmcm*
Calculated density [g/cm^3]	11.35
Crystal size [μm^3]	$20 \times 25 \times 40$
Transm. ratio (max/min)	0.992 / 0.261
Absorption coefficient [mm^{-1}]	102.4
$F(000)$	1084
θ Range [°]	3 to 30
Range in *hkl*	$+6, \pm14, \pm11$
Total no. reflections	1225
Independent reflections	336 ($R_{\rm int} = 0.1012$)
Reflections with $I > 2\sigma(I)$	234 ($R_\sigma = 0.0675$)
Data / parameters	336 / 16
Goodness-of-fit on F^2	0.995
Final R indices [$I > 2\sigma(I)$]	$R1 = 0.0357$
	$wR2 = 0.0569$
R Indices (all data)	$R1 = 0.0668$
	$wR2 = 0.0632$
Extinction coefficient	0.0009(1)
Largest diff. peak and hole [e/Å^3]	3.09 and -2.70

in agreement with the ideal 1:1:2 composition. The large standard uncertainty accounts for different point analyses on the irregularly shaped crystal.

X-ray powder and single crystal data

The purity of the sample was checked through a Guinier powder pattern using Cu-$K_{\alpha1}$ radiation and α-quartz ($a = 491.30$, $c = 540.46$ pm) as an internal standard. The Guinier camera was equipped with an imaging plate system (Fujifilm BAS–1800). The orthorhombic lattice parameters (Table 1) were obtained from a least-squares fit of the Guinier data. To ensure proper indexing, the experimental pattern was compared to a calculated one [7] using the atomic positions obtained from the structure refinement.

Irregularly shaped single crystals of $EuPdTl_2$ were isolated from the annealed sample by mechanical fragmentation and examined by Laue photographs on a Buerger precession camera (equipped with an imaging plate system Fujifilm BAS–1800) in order to establish suitability for intensity data collection. Single crystal intensity data were collected at room temperature by use of a four-circle diffractometer (CAD4) with graphite monochromatized Mo-K_α radiation (71.073 pm) and a scintillation counter with pulse height discrimination. The scans were performed in the $\omega/2\theta$ mode. An empirical absorption correction was applied on the basis of Ψ-scan data followed by a spherical absorption correction.

Table 2. Atomic coordinates and isotropic displacement parameters (pm^2) for $EuPdTl_2$. $U_{\rm eq}$ is defined as one third of the trace of the orthogonalized $U_{\rm ij}$ tensor. The positional parameters determined from the Rietveld refinement are given in italics.

Atom	Wyckoff position	*x*	*y*	*z*	$U_{\rm eq}/B$
Eu	4*c*	0	0.5661(2)	1/4	131(4)
			0.56698(5)		
Pd	4*c*	0	0.2822(2)	1/4	120(5)
			0.28306(7)		
Tl	8*f*	0	0.14490(8)	0.55117(10)	134(3)
			0.14403(3)	*0.55122(5)*	

Table 3. Interatomic distances, calculated with the powder lattice parameters of $EuPdTl_2$. Standard deviations are given in parentheses. All distances within the first coordination spheres are listed.

Eu:	1	Pd	305.7(3)	Tl:	1	Pd	285.7(2)
	2	Pd	322.5(2)		2	Pd	286.5(1)
	4	Tl	341.8(1)		2	Tl	322.9(2)
	2	Tl	350.5(2)		2	Tl	328.6(1)
	4	Tl	357.1(1)		2	Eu	341.8(1)
Pd:	2	Tl	285.7(2)		1	Eu	350.5(2)
	4	Tl	286.5(1)		2	Eu	357.1(1)
	1	Eu	305.7(3)				
	2	Eu	322.5(2)				

All relevant crystallographic data for the data collection and evaluation are listed in Table 1.

Examination of the systematic extinctions of the data set revealed space group *Cmcm*, in agreement with our previous investigations on the indium compounds [8 – 10]. The atomic parameters of $SrPdTl_2$ [4] were taken as starting values and the structure was refined using SHELXL-97 (full-matrix least-squares on F_o^2) [11] with anisotropic atomic displacement parameters for all sites. As a check for possible defects, the occupancy parameters were refined in a separate series of least-squares cycles. All sites were fully occupied within two standard uncertainties. In the final cycles the ideal occupancy parameters were assumed again. A final difference Fourier synthesis revealed no significant residual peaks (see Table 1). The highest residual density was close to the thallium position and most likely resulted from an incomplete absorption correction of this strongly absorbing compound. The positional parameters and interatomic distances are listed in Tables 2 and 3. Further details on the structure refinement are available*.

The bulk sample was also investigated on a powder diffractometer (Stoe Stadi P, Cu-$K_{\alpha1}$ radiation) in order to perform a full profile Rietveld refinement. The data are presented in Fig. 1. The measurement was performed in

*Details may be obtained from: Fachinformationszentrum Karlsruhe, D-76344 Eggenstein-Leopoldshafen (Germany), by quoting the Registry No. CSD–391366.

Table 4. X-ray powder data (Cu-$K_{\alpha1}$) and structure refinement for $EuPdTl_2$.

Unit cell dimensions [pm]	$a = 447.44(3)$
(diffractometer data, Stadi P)	$b = 1079.48(7)$
	$c = 813.23(6)$
Cell volume [nm^3]	$V = 0.3930$
Absorption correction / μR	1.40
Range in 2θ [°]	10 to 100
Scan mode, step width	$\omega/2\theta$, 0.02
No. data points	4751
Total no. Bragg reflections	139
Asymmetry parameters	0.060(5)
	0.0095(7)
No. total parameters	18
R_F, R_{wp}	0.098, 0.303
$R_{Bragg(I)}$, goodness-of-fit, (χ^2)	0.125, 1.375, 2.04
Bérar-Lelann Factor	2.27

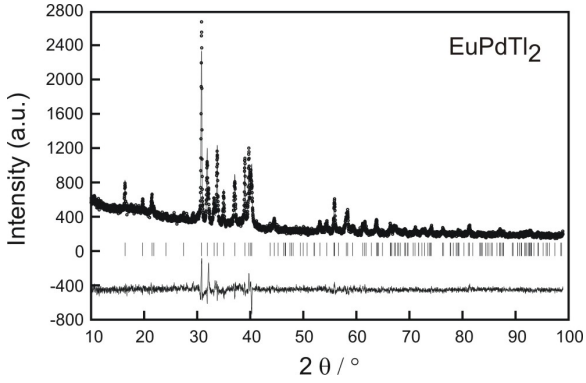

Fig. 1. Rietveld refinement plot for $EuPdTl_2$, in which the observed intensities are indicated with open circles and the calculated pattern with a line on top of the circles. The vertical lines indicate the Bragg positions. The difference I(obs)–I(calc) is drawn below the Bragg indicators.

Debye-Scherrer geometry using Cu-$K_{\alpha1}$ radiation (λ = 154.0598 pm, Ge monochromator). The experimental details are listed in Table 4.

The Rietveld calculation was performed with the FULLPROF [12] software. The background was set manually and the profiles were modelled using the pseudo-Voigt function. An arbitrary absorption value of $\mu R = 1.4$ was used. The experimental data of the three refinements are summarized in Table 4. The standard deviations of the refined parameters have been multiplied with the Bérar-Lelann factor [13]. The resulting positional parameters are listed in Table 2. The powder data fully confirm the $MgCuAl_2$ type structure of $EuPdTl_2$, and we could show that the sample is pure on the level of X-ray powder diffraction.

Property measurements

Magnetic measurements of the polycrystalline powdered sample of $EuPdTl_2$ were determined with an ACMS option

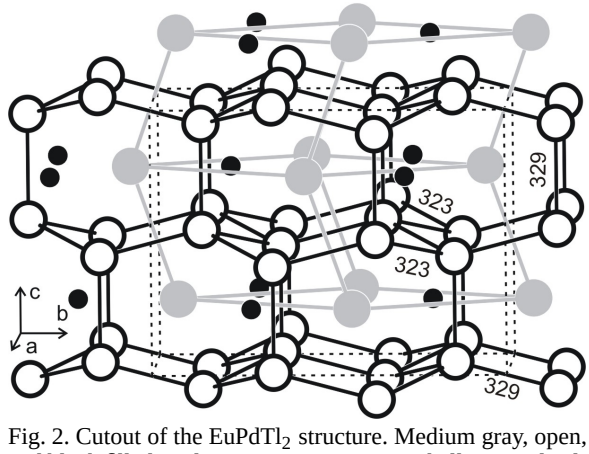

Fig. 2. Cutout of the $EuPdTl_2$ structure. Medium gray, open, and black filled circles represent europium, thallium, and palladium atoms, respectively. Selected bond lengths within the thallium substructure are given in pm.

of the Quantum Design PPMS in the temperature range 3 to 300 K with magnetic flux densities up to 80 kOe. The sample was enclosed in a small gelatin capsule and fixed to the sample holder assembly. While carrying out the susceptibility measurement, the sample was first cooled to 3 K in zero magnetic field and then slowly heated to room temperature in the applied external field of 10 kOe.

The 21.53 keV transition of ^{151}Eu with an activity of 130 MBq (2% of the total activity of a $^{151}Sm{:}EuF_3$ source) was used for a Mössbauer spectroscopic experiment. The measurement was performed with a commercial helium bath cryostat. The temperature of the absorber was kept at 78 K. The source was kept at room temperature. The sample was placed within a thin-walled PVC container at a thickness corresponding to about 10 mg Eu/cm^2.

Discussion

Crystal chemistry

The thallide $EuPdTl_2$ derives from the hexagonal Zintl phase $EuTl_2$ [14] by an insertion of palladium atoms in every other triangle formed by the europium atoms. This insertion results in a strong orthorhombic distortion (Fig. 2). The Zintl-Klemm description of $EuTl_2$, *i. e.* $Eu^{2+}[2Tl^-]$, leaves no electrons for filling of the palladium *d* bands in $EuPdTl_2$. Consequently one needs to oxidize the thallium substructure of $EuTl_2$ in order to realize the charge transfer to the palladium atoms. Indeed we observe an increase of the Tl–Tl distances within the orthorhombically distorted thallium substructure in $EuPdTl_2$ (323 – 329 pm), when compared with $EuTl_2$ (3×299 and 1×328 pm) [14]. The Tl–Tl distances in $EuPdTl_2$, however, are still shorter

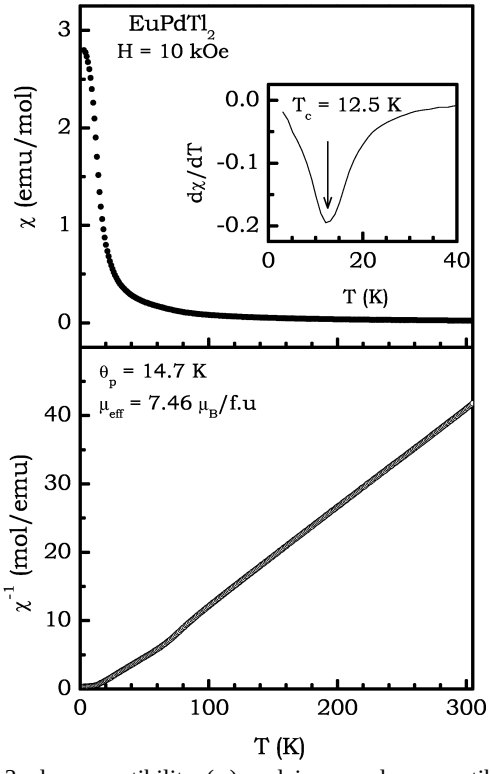

Fig. 3. dc susceptibility (χ) and inverse dc susceptibility (χ^{-1}) as a function of temperature (T) for $EuPdTl_2$, measured in applied field of 10 kOe. The derivative $d\chi/dt$ is shown in the insert.

than the Tl–Tl distances in *hcp* thallium (6×341 and 6×346 pm) [15].

Together, the palladium and thallium atoms build up a three-dimensional $[PdTl_2]$ polyanionic network, where each palladium atom has a strongly distorted trigonal prismatic thallium coordination at Pd–Tl distances of 286 – 287 pm, close to the sum of the covalent radii of 283 pm [16]. The channels left by this network are filled by the europium atoms. The latter have an electrostatic interaction with the $[PdTl_2]$ polyanion through one short Eu–Pd contact at 306 pm. Considering the divalent character of the europium atoms (see below), an ionic formula splitting $Eu^{2+}[PdTl_2]^{2-}$ is a good approximation. Chemical bonding in $EuPdTl_2$ is similar to that of the isotypic indides as well as of $SrPdTl_2$. For details we refer to our previous work [3, 4, 8 – 10].

Physical properties

Already the X-ray data revealed substantial absorption for the $EuPdTl_2$ sample. The collection of reliable

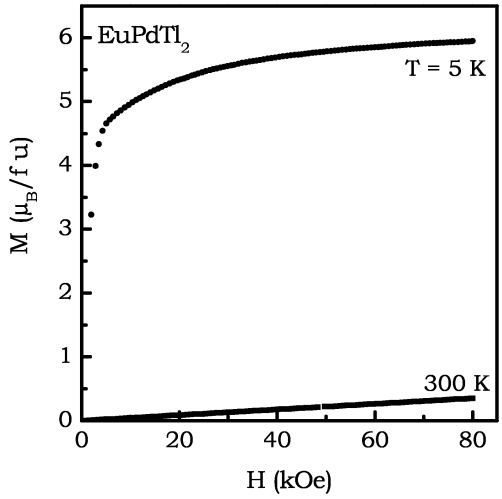

Fig. 4. Magnetization (M) *vs.* applied field (H) for $EuPdTl_2$ at 5 and 300 K.

^{151}Eu Mössbauer spectroscopic data failed due to enormous absorption. Even after ten days of data collection no well resolved Mössbauer signal was available. Determination of the europium valence was therefore based on magnetic data.

The temperature dependence of the magnetic susceptibility of $EuPdTl_2$ is displayed in Fig. 3. In the top panel of the figure, dc susceptibility (χ) is plotted as a function of temperature, measured in a steady field of 10 kOe. χ(T) values raise below 50 K, indicating ferromagnetic like coupling. The first derivative of the susceptibility, $d\chi/dT$ *vs.* T, presented as an insert in Fig. 3, shows the precise Curie temperature (T_C) of 12.5(5) K. In the bottom panel of Fig. 3, we show the inverse susceptibility (χ^{-1}). Above 100 K we observe Curie-Weiss behavior with an experimental magnetic moment of 7.46(5) μ_B/Eu atom, slightly smaller than the free ion value of 7.94 μ_B for Eu^{2+} [17]. Similar magnetic moments have been observed for a variety of equiatomic Eu*TX* intermetallics [18]. Linear extrapolation of the $1/\chi$ *vs.* T curve to $1/\chi = 0$ resulted in a Weiss constant (θ) of 14.7(5) K, indicative of ferromagnetic interactions. The smaller θ/T_C ratio ($= 1.17$) indicates long range magnetic ordering. The small bump in the $1/\chi$ *vs.* T plot around 70 K may be attributed to a very small impurity of ferromagnetic EuO ($T_C = 70$ K) [19, 20], that is frequently observed in europium intermetallics.

The isothermal magnetization (M) behavior is shown in Fig. 4. At room temperature M varies linearly

with H with a magnetic moment of only 0.3 μ_B/Eu as expected for a paramagnetic compound. However at 5 K, well below the Curie temperature, the magnetization steeply increases for small external field strengths and tends towards saturation above 10 kOe. The magnetization at 80 kOe is 5.95 μ_B/Eu, slightly smaller than the theoretical moment of 7 μ_B according to $g \times S$ [17]. According to the magnetization behavior, $EuPdTl_2$ can be classified as a soft ferromagnetic material. Similar magnetization behavior has been observed also for EuMgTl [21], EuAuCd [22], EuAgMg [23], or EuAgCd [24].

Acknowledgements

We thank Dipl.-Chem. F. M. Schappacher for the work at the scanning electron microscope and B. Heying for the intensity data collection. This work was supported by the Deutsche Forschungsgemeinschaft. C.P.S. and S.R. are indebted to the NRW Graduate School of Chemistry and to the Alexander von Humboldt-Stiftung for research grants.

[1] H. Perlitz, A. Westgren, Ark. Kemi, Miner. Geol. **16b**, 1 (1943).
[2] B. Heying, R.-D. Hoffmann, R. Pöttgen, Z. Naturforsch. **60b**, 491 (2005).
[3] R. Pöttgen, M. Lukachuk, R.-D. Hoffmann, Z. Kristallogr., in press.
[4] S. Liu, J. D. Corbett, Inorg. Chem. **42**, 4898 (2003).
[5] R. Pöttgen, Th. Gulden, A. Simon, GIT Labor Fachzeitschrift **43**, 133 (1999).
[6] D. Kußmann, R.-D. Hoffmann, R. Pöttgen, Z. Anorg. Allg. Chem. **624**, 1727 (1998).
[7] K. Yvon, W. Jeitschko, E. Parthé, J. Appl. Crystallogr. **10**, 73 (1977).
[8] R.-D. Hoffmann, U. Ch. Rodewald, R. Pöttgen, Z. Naturforsch. **54b**, 38 (1999).
[9] Ya. V. Galadzhun, R.-D. Hoffmann, G. Kotzyba, B. Künnen, R. Pöttgen, Eur. J. Inorg. Chem. 975 (1999).
[10] R.-D. Hoffmann, R. Pöttgen, Chem. Eur. J. **7**, 382 (2001).
[11] G. M. Sheldrick, SHELXL-97, Program for Crystal Structure Refinement, University of Göttingen, Germany (1997).
[12] T. Roisnel, J. Rodríguez-Carvajal, Fullprof.2k V. 2.0 (2001) Laboratoire Léon Brillouin (CEA-CNRS), 91191 Gif-sur-Yvette Cedex (France).
[13] J.-F. Bérar, P. Lelann, J. Appl. Crystallogr. **24**, 1 (1991).
[14] A. Iandelli, Z. Anorg. Allg. Chem. **330**, 221 (1964).
[15] J. Donohue, The Structures of the Elements, Wiley, New York (1974).
[16] J. Emsley, The Elements, Oxford University Press, Oxford (1999).
[17] H. Lueken, Magnetochemie, Teubner, Stuttgart (1999).
[18] R. Pöttgen, D. Johrendt, Chem. Mater. **12**, 875 (2000).
[19] B. D. McWhan, P. C. Souers, G. Jura, Phys. Rev. **143**, 385 (1966).
[20] B. Stroka, J. Wosnitza, E. Scheer, H. von Löhneysen, W. Park, K. Fischer, Z. Phys. Condens. Matter **89**, 39 (1992).
[21] R. Kraft, R.-D. Hoffmann, C. P. Sebastian, R. Pöttgen, Yu. Grin, Yu. M. Prots', W. Schnelle, M. Schmidt, M. Baitinger, Chem. Mater., to be submitted.
[22] R. Mishra, R. Pöttgen, R.-D. Hoffmann, D. Kaczorowski, H. Piotrowski, P. Mayer, C. Rosenhahn, B. D. Mosel, Z. Anorg. Allg. Chem. **627**, 1283 (2001).
[23] D. Johrendt, G. Kotzyba, H. Trill, B. D. Mosel, H. Eckert, Th. Fickenscher, R. Pöttgen, J. Solid State Chem. **164**, 201 (2002).
[24] Th. Fickenscher, G. Kotzyba, R.-D. Hoffmann, R. Pöttgen, Z. Naturforsch. **56b**, 598 (2001).